A Techno-Economic Assessment of Wind Power Expansion with Battery Storage Under Wind Energy Uncertainty

Bui Xuan Luc
Faculty of Electrical and Electronics Engineering, Ho Chi Minh City University of Technology and Education, Ho Chi Minh City, Vietnam
lucbx25.ncs@hcmute.edu.vn

Dinh Ngoc Sang
Faculty of Electrical and Electronics Engineering, Ho Chi Minh City University of Technology and Education, Ho Chi Minh City, Vietnam | Department of Urban Engineering, University of Architecture Ho Chi Minh City, Ho Chi Minh City, Vietnam
sangdn.ncs@hcmute.edu.vn

Truong Viet Anh
Faculty of Electrical and Electronics Engineering, Ho Chi Minh City University of Technology and Education, Ho Chi Minh City, Vietnam
anhtv@hcmute.edu.vn (corresponding author)

Received: 18 May 2025 | Revised: 25 August 2025 | Accepted: 30 August 2025

 DOI: https://doi.org/10.48084/etasr.12229

ABSTRACT

The techno-economic performance of novel wind power investment projects is significantly influenced by the inherent uncertainty of the power production. Additionally, challenges associated with land clearance and compensation, which are required to develop transmission infrastructure to accommodate additional wind capacity in the national grid, are also present. This study investigates capacity expansion strategies for wind farms that do not require modifications to the existing infrastructure. It focuses on the optimization of intermediate Turbine Control System (TCS) operations and the integration of Battery Energy Storage Systems (BESS). The Harris Hawks Optimization (HHO) algorithm is employed to determine the optimal BESS size to enhance the overall system performance and maximize the investment returns. Specifically, BESS charge/discharge power limits are configured to ensure that the TCS output remains both controllable and stable, while also extending the operational lifespan of the BESS under highly variable wind conditions. The experimental results indicate that integrating BESS into wind farm expansion strategies not only enables more effective bidding in competitive electricity markets, but also ensures compliance with grid technical standards, in addition to superior economic performance compared to previously published methods.

Keywords-wind power; uncertain; Bess; transformer; net present value

I. INTRODUCTION

Wind energy has experienced a growth in the installed capacity as a pivotal renewable energy source in the transition toward sustainable electricity systems [1]. According to [2], the wind energy significance is increasing. Numerous countries, including China, the United States of America, and Southeast Asian nations, are actively investing in this sector [3, 4]. The transition towards wind energy faces obstacles, such as considerable initial investment requirements, variability in the power output, and diminished governmental participation.

Numerous studies address the negative effects of the inherent uncertainty in wind power production. Three prominent directions include the accurate power output forecasting, optimization of integrated operational models, and the integration of BESS. Authors in [5] utilized AI techniques for a more precise wind speed forecasting. An enhanced Particle Swarm Optimization (PSO) algorithm hybridized with Long Short-Term Memory (LSTM) was employed to optimize the integrated wind–thermal power plant model for bidding in the electricity market [6]. Authors in [7] explored BESS to enhance the efficiency of wind farm utilization.

Studies integrating BESS to enhance the performance of wind power systems are summarized in Table I. Previous studies focused on the BESS optimization of operation, sizing, or examination of the impact of the wind power on equipment. There is no identified research that simultaneously addressed the utilization of the available capacity of substations and integration of BESS in a comprehensive economic–technical framework for peak and off-peak periods. This study provides a plan to increase the wind power facilities without an infrastructure upgrade, using an optimized BESS model to ensure grid stability and reduce costs. The BESS model has a transformer control that ensures the power stability, protects the equipment, extends the BESS life, and provides revenue assurance.

TABLE I. COMPARATIVE ANALYSIS WITH PREVIOUS STUDIES

Reference	IEEE system	TCS	Wind uncertain	Design BESS	Capacity degradation	Profit	Investments	Optimization algorithm
[8]	14 Bus	x	✓	✓	x	✓	x	x
[9]	x	x	x	✓	x	x	x	x
[10]	x	x	x	✓	✓	x	x	✓
[11]	x	✓	✓	x	x	x	x	x
[12]	x	✓	✓	x	x	✓	✓	x
[13]	30 Bus	x	✓	✓	x	✓	x	x
Present Study	30 Bus	✓	✓	✓	✓	✓	✓	✓

II. MATHEMATICAL MODEL

Previous studies have focused on the financial aspects of wind turbines, while investments in TCS have received less attention, even though they account for 7-10% of the total cost, according to [14]. Although this percentage is small, it directly impacts the profitability, power losses, system reliability, and stability. This study analyzes the impact of TCS investment on the economic performance of wind farms. The proposed model optimizes the joint operation of a wind farm and BESS, explicitly considering the degradation costs during discharging. The objective function maximizes the Net Present Value (NPV) of the system. The seasonal variations in wind power are modeled using probability distributions for both high-wind and low-wind seasons. HHO is employed to determine the optimal BESS size that yields maximum NPV. To provide a comprehensive evaluation, four scenarios are examined: (a) baseline wind farm, (b) wind farm with BESS, (c) wind farm with expanded capacity without upgrading the TCS infrastructure, and (d) expanded wind farm with BESS but without upgrading the TCS infrastructure. This integrated framework allows both the role of TCS investment and the long-term economic feasibility of wind–BESS systems to be assessed.

A. Wind Farm TCS

The rated capacity of conventional TCS is determined according to International Electrotechnical Commission (IEC) standards, based on the wind power capacity transmitted through it [15]. The TCS capacity directly affects the investment costs, scalability, and the long-term economic performance of the Wind Power Plant (WPP). The selected capacity must ensure stable operation, the ability to withstand prolonged overload, and respond to short-term overloading events. An example of TCS investment and operational costs in Sweden is provided in [12]. Optimizing the TCS capacity is essential to balance the transmission capability with the technical constraints, thereby enhancing the overall efficiency of the project. Under these standards, the TCS design considers the operating temperature conditions and expected service life.

1) Transformer Temperature Limits

The temperature at various locations within a transformer significantly affects the lifespan of insulation and conductive materials. Under operating conditions, including both long-term and short-term overloads, the hot-spot temperature and top-oil temperature limits must be maintained within acceptable thresholds:

$$\theta_t^{hst} \le \theta_t^{hst,max} \quad (1)$$

$$\theta_t^{top} \le \theta_t^{top,max} \quad (2)$$

where θ_t^{hst} is the hot-spot winding temperature and θ_t^{top} is the top-oil temperature. Both variables are directly influenced by the operating power level of the transformer [15].

2) Lifetime Limit

A key parameter for transformers is the Loss of Life (LOL), which indicates the hourly rate of accumulated aging of the transformer presented by [15]:

$$LOL = \sum_t^T V_t \quad (3)$$

After determining the aging rate, the LOL index can be calculated using (3), as per the specified standards. To ensure that the transformer does not fail before the WPP reaches the end of its lifecycle, the upper limit of LOL is set to match the operational lifespan of the wind farm, as described in:

$$LOL \le \frac{Transformer's\ Lifetime}{Wind\ Farm's\ Lifetime} . 8760 \quad (4)$$

B. Wind Revenue

In the electricity market, ensuring the stability of the power system is a persistent issue when the WPP model is integrated into the power system. To address this, the profit from electricity sales is considered a random variable with uncertainty, and in this case, it is determined through:

$$R_t = \sum_{t=1}^T R_{bid}\left(P_t^{bid}\right) + \sum_{t=1}^T R_{prob}(\Delta P_t^{wp}) \quad (5)$$

where $\Delta P_t^{wp} = P_t^{prob} - P_t^{bid}$, R_{bid} represents the bidding revenue of the WPP to the ISO, and R_{prob} represents the revenue from the uncertainty of the WPP, considering the probability distribution fluctuations based on P_t^{bid} [15].

1) Bidding Income

$$R_{bid} = \sum_{t=1}^{T} \lambda_w . P_t^{bid} \quad (6)$$

where λ_w is the selling price of the WPP's capacity. The revenue from WPP's bidding is calculated as the total revenue at various time points. This electricity price is significantly influenced by the electricity market.

2) Probabilistic Revenue

This revenue comprises surplus capacity sales and penalties for power shortages, as defined in (8) and (9). While the surplus capacity can be sold at a reduced price in some studies, this paper prioritizes the grid stability, curtailing excess output instead. Power shortages incur penalties at twice the standard electricity price. The uncertainty in revenue is represented by:

$$R_{prob} = \begin{cases} \sum_{t=1}^{T} R_{sur}\left(\Delta P_t^{wp}\right), \ if \ \Delta P_t^{wp} \geq 0 \\ \sum_{t=1}^{T} C_{pen}\left(\Delta P_t^{wp}\right), \ if \ \Delta P_t^{wp} < 0 \end{cases} \quad (7)$$

where R_{sur} denotes the revenue earned from selling surplus wind power generation.

$$R_{Rw}(\Delta P_t^{w}) = k_R . \lambda_w . \Delta P_t^{wp}$$
$$= k_R . \lambda_t . \int_{P_t^{bid}}^{P^{wr}} \left(p_t^{wp} - P_t^{bid}\right) . f_w\left(p_t^{wp}\right) . dp_t^{wp} \quad (8)$$

And the penalty cost C_{pen} for the wind power deficit is expressed by:

$$C_{pen}\left(\Delta P_t^{wp}\right) = k_P . \lambda_t . \Delta P_t^{wp}$$
$$= k_P . \lambda_t . \int_{0}^{P_t^{bid}} \left(p_t^{wp} - P_t^{bid}\right) . f_w\left(p_t^{wp}\right) . dp_t^{wp} \quad (9)$$

where $k_R . \lambda_t$ is the reserve pricing and k_R is the reserve price coefficient. Similarly, compensation pricing is expressed as $k_P . \lambda_t$, with k_P being the compensation coefficient. The rated wind power capacity is denoted by P^{wr}.

The analysis employs a Weibull probability density function to model the wind speed effects. Among the probability distributions, the two-parameter Weibull function is the most widely adopted. The wind speed frequency model follows the specifications of [16]. The active power output of an Enercon E82-E4 turbine (rated 3MW) is determined through the wind-speed-to-power conversion, as detailed in [17].

C. BESS Model

BESS stores renewable energy and discharges to balance the supply and demand. They enhance the grid stability by mitigating weather-induced power fluctuations, improving the power quality, and reducing the reliance on traditional generation. With rapid response capabilities, BESS provide frequency regulation and ancillary services, accelerating the transition to smart grids [18]. Lithium-ion batteries currently dominate BESS applications due to their efficiency (80-90%) and operational flexibility [19, 20]. They are preferred as contemporary energy storage solutions due to their balanced performance and declining costs. In [21], it was noted that the investment cost of BESS depends on its duration scaling factor. The annual operation and maintenance cost typically accounts for approximately 1–3% of the total capital investment [20].

The simulation model integrates a BESS to reflect real-world performance with capacity degradation driven by calendar and cycle aging [22]. Cycle aging or cycle degrade, based on the usage frequency and C-rate, is quantified using the depth of discharge $SOC\ (t) - SOC\ (t-1)$ and $C - rate$ [23]. The BESS minimize the excess power curtailment and penalty costs from shortages, discharging only when the economic benefit outweighs the degradation costs as described by:

$$R_{t,BESS} - R_t \geq Cycle\ degrade \quad (10)$$

where $R_{t,BESS}$ is the wind power revenue with BESS. At each time step, the system is constrained to either charge or discharge, depending on the State of Charge (SOC) and operational constraints.

$$Cycle\ degrade = -\Delta SOC * 3.57 * 10^{-5} * e^{0.465 * C-rate} \quad (11)$$

The charging energy (E_{cha}) and discharging energy (E_{dis})are represented by:

$$E_{cha} = P_{cha} . t \quad (12)$$

$$E_{dis} = P_{dis} . t \quad (13)$$

Additionally, P_{cha}, P_{dis} are the charging and discharging power of the BESS, respectively.

$$P_{cha} = \int_{P_t^{bid}}^{P^{wr}} \left(p_t^{wp} - P_t^{bid}\right) . f_w\left(p_t^{wp}\right) . dp_t^{wp} \quad (14)$$

$$P_{dis} = \int_{0}^{P_t^{bid}} \left(p_t^{wp} - P_t^{bid}\right) . f_w\left(p_t^{wp}\right) . dp_t^{wp} \quad (15)$$

III. METHODOLOGY

A. HHO Algorithm

The study uses HHO to optimize the BESS capacity and rated discharge power, assuming equal charging and discharge rates. The algorithm mimics Harris hawks' hunting behavior with two primary phases [24]. During the exploration phase when $|E| \geq 1$, the hawk searches randomly, according to (16), for q greater or equal to 0.5, and according to (17), for the rest of the cases.

$$X_{HHO}(t+1) = X_{rand}(t) - r_1 |X_{rand}(t) - 2 r_2 X(t)| \quad (16)$$

$$X_{HHO}(t+1) = X_{rabbit}(t) - X_m(t) - r_3(LB + r_4(UB - LB)) \quad (17)$$

where $X_{rand}(t)$ is the random position of a hawk in the population, $X_m(t)$ is the average position of the population calculated by (18), r is a random number between 0 and 1. The prey energy is calculated by:

$$X_m(t) = \frac{1}{N} \sum_{i=1}^{N} X_i(t) \quad (18)$$

$$E = 2 . E_0 \left(1 - \frac{t}{T}\right) \quad (19)$$

where E_0 is the initial energy with random in the range of -1 to 1, t is the current iteration, and T is the maximum number of iterations.

During the exploitation phase when $|E| < 1$, the hawk attacks the prey with four strategies:

- Soft besiege ($r \geq 0.5$ and $|E| \geq 0.5$):

$$X_{HHO}(t+1) = \Delta X - E \cdot |J \cdot X_{rabbit}(t) - X(t)| \quad (20)$$

where $\Delta X = X_{\text{rabbit}} - X(t)$, $J = 2.(1-r)$ is the strength of the jump, and r is a random number between 0 and 1.

- Hard besiege ($r \geq 0.5$ and $|E| < 0.5$):

$$X_{HHO}(t+1) = X_{\text{rabbit}}(t) - E \cdot |\Delta X(t)| \quad (21)$$

- Soft besiege with progressive rapid dives ($r < 0.5$ and $|E| \geq 0.5$):

$$Y = X_{rabbit}(t) - E \cdot |J \cdot X_{rabbit}(t) - X(t)| \quad (22)$$

$$Z = Y + S \cdot LF \quad (23)$$

where S is the random vector, LF is the Levy Flight, calculated by:

$$LF = 0.01.\frac{u.\sigma}{|v|^{1/\beta}}, \sigma = \left(\frac{\Gamma(1+\beta).\sin\left(\frac{\pi\beta}{2}\right)}{\Gamma\left(\frac{1+\beta}{2}\right).\beta.2^{\frac{(\beta-1)}{2}}}\right)^{1/\beta} \quad (24)$$

where u and v are random numbers from a normal distribution and $\beta = 1.5$. The X_{HHO} is chosen, as described by:

$$X_{HHO}(t+1) = \begin{cases} Y, & if\ F(Y) > F(X(t)) \\ Z, & if\ F(Z) > F(X(t)) \end{cases} \quad (25)$$

- Hard besiege with progressive rapid dives ($r < 0.5$ and $|E| < 0.5$):

$$Y = X_{rabbit}(t) - E. |J. X_{rabbit}(t) - X_m(t)| \quad (26)$$

$$Z = Y + S \cdot LF \quad (27)$$

where X_{HHO} will be chosen as in:

B. Fitness Function

In a WPP project, the important criterion considered is NPV. This indicator is determined by:

$$\max NPV = \sum_{t=1}^{T} \frac{Z_t}{(1+r)^t} - I_s \quad (28)$$

where Z_t is the net cash flow at time t, calculated using (29). T represents the expected lifetime of the WPP, which is assumed to be 20 years [12]. The discount rate or interest rate is denoted by r:

$$Z_t = R_t - C_t + G_t \quad (29)$$

where R_t is the bidding revenue of the WPP, C_t is the operation and maintenance cost, and G_t refers to green certificates that generate additional revenue and certify the electricity production from renewable sources. The registration fee in 2019 was 0.305 €/MWh, as reported in [12].

The initial investment cost I_s encompasses wind turbine procurement, infrastructure construction, substation installation, transportation, commissioning, and grid connection. This cost critically impacts the financial feasibility, payback period, capital requirements, and revenue optimization potential.

IV. EXPERIMENT

Four wind power scenarios were simulated within the IEEE 30-bus system in this study. Scenario 1 included Baseline Wind Power Configuration (BWPC): the baseline WPP model. Scenario 2 included the expanded Capacity Wind Power Configuration (CWPC): an extended turbine capacity model utilizing the existing infrastructure. Scenario 3 involved BWPC with BESS: integration of BESS into the baseline system. Scenario 4 entailed CWPC and BESS: a combination of BESS with expanded wind farm capacity while maintaining the original infrastructure.

A. Input Data

The IEEE 30-bus system consists of 30 buses, 40 branches, and 6 generating units. The system parameters are available in [25]. Two wind farms replace conventional generators at buses 5 and 11. The wind farm at bus 5 is modeled after Weibull parameters c=9, k=2, and wind farm at bus 11 with c=10, k=2 according to [17]. The reference parameters and the Weibull probability density function are provided in [26], as shown in Figure 1(a).

1) WPP

The economic cost depends on technology, location, and support policies. The estimated investment cost is around 950,000 €/MW, excluding Operations and Maintenance (O&M), with a lifespan of 20 years [27]. The annual O&M cost accounts for approximately 1.5% of the investment capital. The profitability is influenced by the conventional electricity prices in the market.

This study examines the problem for a WPP at bus 5 using forecasted wind data from both peak and low seasons [26]. Specifically, the low season, which typically occurs in May, June, and July, shows a predicted wind power output as illustrated in Figure 1 [5]. The predicted wind energy is displayed, including hourly forecast errors, in two seasons with probability bands for the energy levels per time step

2) TCS

To evaluate the optimization problem, a medium-capacity transformer is selected. The initial investment is assumed to be 1,782,608 €, and the O&M cost for the transformer is estimated at 1.5% of the investment [12]. The thermal parameters for the transformers are assumed to be the same, with the TCS parameters for insulation using ODAF [15].

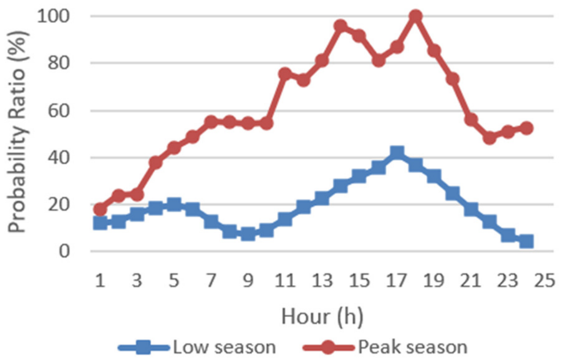

(a)

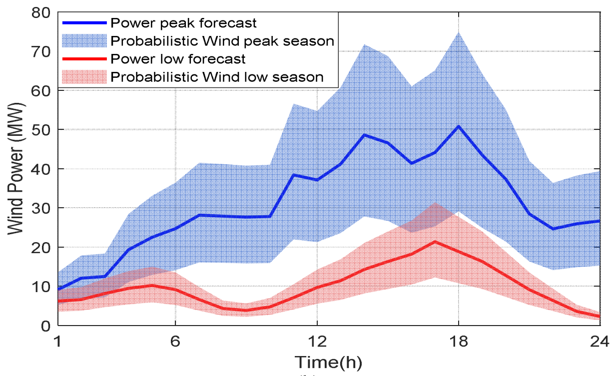

(b)

Fig. 1. (a) Probability ration and (b) wind power output of forecasted wind energy in peak and low seasons in bus 5.

3) *BESS*

This experiment employs lithium-based technology for the BESS. The O&M costs account for 3% of the total capital investment and an investment cost ranging between 164 and 211 USD/kWh [20, 21]. Both charging and discharging efficiencies are assumed to be 95%, yielding an overall round-trip efficiency of about 90%. The degradation factor due to aging is adopted from [22], as in (10), while the charge/discharge operating range is taken as 0–100% SoC [23]. Although this range is theoretically 0–100%, the practical operation is typically restricted to about 30–90% SoC due to the efficiency losses and degradation effects during charging/discharging.

B. *Results*

1) *Scenario 1- BWPC*

Following the IEC standard, the TCS power is calculated to meet the 57 MVA requirement of the WPP and is selected as 63 MVA. Figure 2a depicts the variation in the Hot Spot and Top Oil temperatures of the TCS, which fluctuate based on the maximum possible power over a 24-h period to support the evaluation and selection of the appropriate TCS rating.

2) *Scenario 2- CWPC*

Figure 2(a) indicates that the peak TCS temperature remains below the critical limit. Furthermore, the peak temperature occurs with a relatively low probability during the short time frame of 18:00–19:00 on peak days. Consequently, the wind power capacity can be increased to optimize the TCS operating conditions. In Scenario 2, the rated wind capacity is expanded by an additional 15 MW while still ensuring the TCS temperature and lifespan requirements. The results are illustrated in Figure 2(b).

3) *Scenario 3- BWPC with BESS*

The BESS is integrated in this third scenario. The BESS optimization problem is also solved using the HHO algorithm. Following the integration of BESS, the operating temperature profile of the TCS has changed, as portrayed in Figure 2(c).

4) *Scenario 4- CWPC with BESS*

This scenario involves both the expansion of the wind power capacity and the integration of a BESS. The BESS operates in two complementary modes: (a) storing the portion of wind energy that statistically exceeds the transmission capacity of TCS or the committed bidding quantity, and (b) discharging to compensate for potential shortfalls in wind generation relative to the bidding commitment. Under these operating modes, the variation in TCS operating temperature is presented in Figure 2(d).

V. DISCUCCION

A. *Technical Evaluation*

A unified techno-economic model has been successfully implemented. The model integrates wind power sources with transmission infrastructure to supply electricity to the standard IEEE 30-bus system. A key technical challenge addressed in this setup is that while the rated wind capacity is inherently expandable, the transmission capacity remains fixed. Subsequently, the power system requires maintaining the operational stability under variable input conditions. Figure 2 illustrates the operation of the TCS, a critical interface that enables the flow of wind-generated power into the electricity market, under four distinct scenarios.

Scenarios 2 and 4 exhibit that the wind capacity may be expanded up without a transmission infrastructure upgrade since the high wind generation is not a frequent occurrence. In Scenario 2, this may be transformer overloading, which causes curtailment, while in Scenario 4, curtailment is avoided by storing the surplus energy in BESS. Additionally, BESS (Scenario 3) reduces the TCS thermal stress during times of unstable wind, extending the equipment life, and in Scenario 4, it also increases the stability and continuity of the wind energy utilization.

B. *Economical Evaluation*

The economic performance of the tested scenarios is summarized in Table II and is compared to other studies. The results indicate that the integration of BESS enhances the economic efficiency compared to other configurations, particularly in scenarios involving wind power expansion. Specifically, for the same wind capacity invested, the NPV in Scenario 2 increases from 4.29 million to 7.72 million €, while Scenario 4 achieves the highest NPV of 13.61 million €, corresponding to the highest capital efficiency of over 151,000 €/MW.

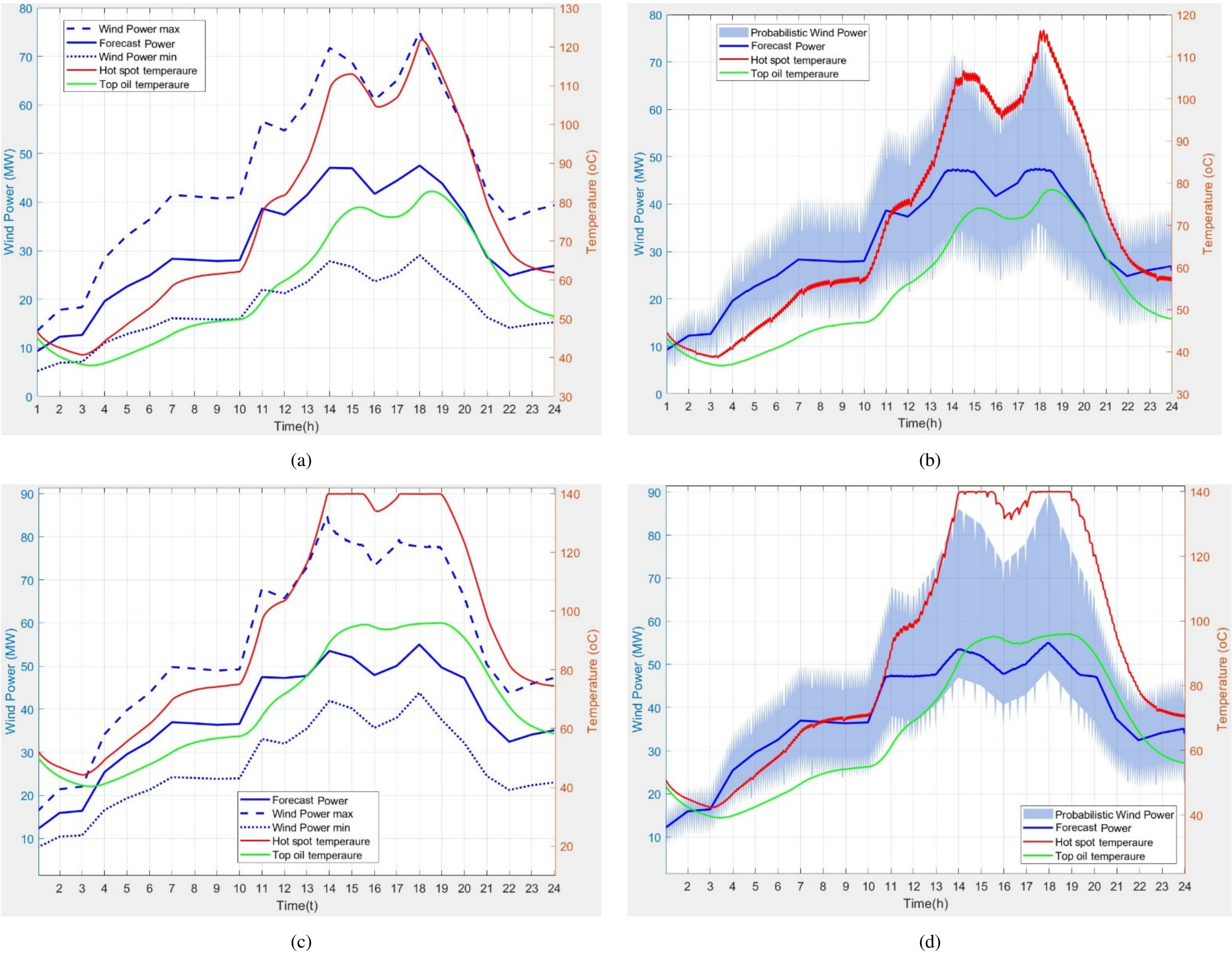

Fig. 2. The operation temperature of the transformer under wind power output variation for (a) Scenario 1, (b) Scenario 2, (c) Scenario 3, and (d) Scenario 4.

TABLE II. ECONOMIC PERFORMANCE

Option	**BWPC**	**CWPC**	**BWPC with BESS**	**CWPC with BESS**	**[8]**	**[13]**		**[28]**
Bus	5	5	5	5	6	23	13	5
IEEE system	30 Bus	30 Bus	30 Bus	30 Bus	14 Bus	30 Bus		30 Bus
Wind power rated (MW)	75	90	75	90	85	30	10	90
Transformer size (MVA)	63	63	63	63	No	No		63
Storage battery (MWh)	No	No	84	72	160	136.57		140
NPV (M€)	4.29	10.58	7.72	13.61	No	No		17.28
NPV/P_{rated}(k€/MW)	57.2	117.56	102.93	151.22	70.6	0.72		192

Figure 3 illustrates the NPV value of each under-study scenario under escalating penalty factors (K_p). In scenarios lacking BESS integration (Scenarios 1 and 2), as K_p increases, NPV presents the opposite behavior. This is attributed to the inability to adjust the power output to mitigate penalties. Specifically, in BWPC scenario, NPV decreases from 7.76 million € ($K_p = 1.5$) to -2.39 million € at $K_p = 4$, reflecting severe financial vulnerability. Similarly, in CWPC scenario, its NPV decreases from 13.26 million to 5.14 million €, while it is considered more robust. In contrast, BESS-integrated scenarios demonstrate superior resilience. Particularly, CWPC-BESS scenario maintains a positive NPV of 9.45 million € ($K_p = 4$). In Scenario 3, a decrease from 9.85 million to 2.43 million € is observed. However, it still outperforms its non-BESS counterpart by avoiding the negative returns. It is evident that the revenue streams are stabilized from BESS's capacity to buffer against financial penalties by enabling a better alignment of the power delivery with forecasts.

The results of the present study are compared to the literature under the same operating conditions as in [8, 13, 28]. The investment payback per MW of wind power in Scenario 3

(102.93 k€/MW) and Scenario 4 (151.22 k€/MW) is substantially higher than [8] (70.6 k€/MW) and [13] (0.72 k€/MW). In addition, the same variable is marginally lower compared to [28] (192 k€/MW) although the penalty costs associated with the wind power shortfall in the electricity market were not incorporated. This absence is a factor that can constitute a considerable proportion of the wind power revenues when participating in a competitive market [8]. Furthermore, the effectiveness of the storage system in the present study (72–84 MWh) clearly outperforms the one of [28] (140 MWh). Moreover, the present study ensures adequate compensation for the wind power deficits under a penalty rate 1.5 times higher than the standard. This superior performance can be attributed to the proposed methodology, which enables the optimal exploitation of the transformer operation under wind power uncertainty, as elaborated in the methodology section above.

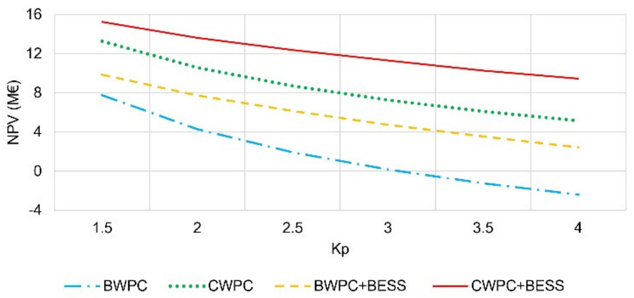

Fig. 3. NPV of the each scenario under penalty.

VI. CONCLUSION

The current study provides a comprehensive techno-economic evaluation of wind energy investment strategies. It proposes an effective solution for optimizing the wind farm development. The results confirm that integrating Battery Energy Storage Systems (BESS) into the operational framework of Turbine Control System (TCS) can significantly enhance the transmission efficiency of the wind power. In addition, it ensures compliance with technical constraints, thereby enabling the scalable expansion of existing wind farms. Among the four evaluated scenarios, the one including Capacity Wind Power Configuration (CWPC) and BESS configuration demonstrates the highest economic benefit, reinforcing its potential as a strategic model within the broader context of green energy transition. Furthermore, the application of the Harris Hawks Optimization (HHO) algorithm shows superior performance in determining both the optimal expansion capacity and BESS sizing, outperforming previously reported methods in terms of capital efficiency and investment effectiveness. Further studies are still required through experiments comparable to recent works,

REFERENCES

[1] International Renewable Energy Agency, *Renewable Energy and Climate Pledges*. Abu Dhabi, UAE: International Renewable Energy Agency, 2020.

[2] International Energy Agency, *Renewables 2024 Analysis and Forecast To 2030*. Paris, France: Renewables 2024 Analysis and Forecast To 2030, 2024.

[3] International Renewable Energy Agency, *Future of Wind: Deployment, Investment, Technology, Grid Integration and Socio-Economic Aspects*. Abu Dhabi, UAE: International Renewable Energy Agency, 2019.

[4] G. M. Idroes, I. Hardi, Md. H. Rahman, M. Afjal, T. R. Noviandy, and R. Idroes, "The dynamic impact of non-renewable and renewable energy on carbon dioxide emissions and ecological footprint in Indonesia," *Carbon Research*, vol. 3, no. 1, Apr. 2024, Art. no. 35, https://doi.org/10.1007/s44246-024-00117-0.

[5] K. Kumar, P. Prabhakar, A. Verma, S. Saroha, and K. Singh, "Advancements in wind power forecasting: A comprehensive review of artificial intelligence-based approaches," *Multimedia Tools and Applications*, vol. 84, no. 10, pp. 8331–8360, Mar. 2025, https://doi.org/10.1007/s11042-024-18916-3.

[6] V. A. Truong, N. S. Dinh, T. L. Duong, N. T. Le, C. D. Truong, and L. T. Nguyen, "Hybrid LSTM-PSO optimization techniques for enhancing wind power bidding efficiency in electricity markets," *Ain Shams Engineering Journal*, vol. 16, no. 2, Feb. 2025, Art. no. 103285, https://doi.org/10.1016/j.asej.2025.103285.

[7] M. Gwabavu, R. C. Bansal, and R. M. Naidoo, "A review of onshore wind farm battery energy storage systems for techno-economic optimization," *International Journal of Modelling and Simulation*, vol. 0, pp. 1–20, Feb. 2024, https://doi.org/10.1080/02286203.2024.2320583.

[8] N. T. A. Nguyen and D. D. Le, "Day-ahead Coordinated Operation of a Wind-Storage System Considering Wind Forecast Uncertainty," *Engineering, Technology & Applied Science Research*, vol. 11, no. 3, pp. 7201–7206, June 2021, https://doi.org/10.48084/etasr.4176.

[9] V. A. Vaishampayan, T. Antony, and A. Yogarathnam, "Effective Capacity of a Battery Energy Storage System Captive to a Wind Farm," in *Proceedings of IEEE PES Grid Edge Technologies Conference & Exposition (Grid Edge)*, San Diego, CA, USA, 2025, https://doi.org/10.1109/GridEdge61154.2025.10887505.

[10] R. Sakipour and H. Abdi, "Optimizing Battery Energy Storage System Data in the Presence of Wind Power Plants: A Comparative Study on Evolutionary Algorithms," *Sustainability*, vol. 12, no. 24, Aug. 2020, Art. no. 10257, https://doi.org/10.3390/su122410257.

[11] M. Fantauzzi, D. Lauria, F. Mottola, and D. Proto, "Estimating Wind Farm Transformers Rating through Lifetime Characterization Based on Stochastic Modeling of Wind Power," *Energies*, vol. 14, no. 5, Sept. 2021, Art. no. 1498, https://doi.org/10.3390/en14051498.

[12] A. Molina Gómez, K. Morozovska, T. Laneryd, and P. Hilber, "Optimal sizing of the wind farm and wind farm transformer using MILP and dynamic transformer rating," *International Journal of Electrical Power & Energy Systems*, vol. 136, Nov. 2021, Art. no. 107645, https://doi.org/10.1016/j.ijepes.2021.107645.

[13] R. Ansaripour, H. Barati, and A. Ghasemi, "A chance-constrained optimization framework for transmission congestion management and frequency regulation in the presence of wind farms and energy storage systems," *Electric Power Systems Research*, vol. 213, Aug. 2022, Art. no. 108712, https://doi.org/10.1016/j.epsr.2022.108712.

[14] S. Alsubal, W. S. Alaloul, E. L. Shawn, M. S. Liew, P. Palaniappan, and M. A. Musarat, "Life Cycle Cost Assessment of Offshore Wind Farm: Kudat Malaysia Case," *Sustainability*, vol. 13, no. 14, July 2021, Art. no. 7943, https://doi.org/10.3390/su13147943.

[15] *International Standards: Power transformers – Part 7: Loading guide for mineral-oil-immersed power transformers*, IEC 60076-7, International Electrotechnical Commission, Geneva, Switzerland, 2018.

[16] J. V. Seguro and T. W. Lambert, "Modern estimation of the parameters of the Weibull wind speed distribution for wind energy analysis," *Journal of Wind Engineering and Industrial Aerodynamics*, vol. 85, no. 1, pp. 75–84, Feb. 2000, https://doi.org/10.1016/S0167-6105(99)00122-1.

[17] P. P. Biswas, P. N. Suganthan, and G. A. J. Amaratunga, "Optimal power flow solutions incorporating stochastic wind and solar power," *Energy Conversion and Management*, vol. 148, pp. 1194–1207, Apr. 2017, https://doi.org/10.1016/j.enconman.2017.06.071.

[18] T. L. Nguyen, N. S. Dinh, V. A. Truong, T. L. Duong, D. H. Du, and D. A. Tuan, "Enhancing Total Transfer Capability via Optimal Location of Energy Storage Systems Using a Hybrid Improved Min-Cut Algorithm and Genetic Algorithm," in *Lecture Notes in Networks and Systems*,

Cham, Switzerland, 2023, vol. 602, pp. 512–524, https://doi.org/10.1007/978-3-031-22200-9_57.

[19] B. Dunn, H. Kamath, and J.-M. Tarascon, "Electrical Energy Storage for the Grid: A Battery of Choices," *Science*, vol. 334, no. 6058, pp. 928–935, Nov. 2011, https://doi.org/ 10.1126/science.1212741.

[20] K. Mongird *et al.*, "Energy Storage Technology and Cost Characterization Report," Pacific Northwest National Laboratory, Richland, WA, USA, Technical Report 28866, July 2019, https://doi.org/10.2172/1573487.

[21] V. Ramasamy *et al.*, "U.S. Solar Photovoltaic System and Energy Storage Cost Benchmarks, With Minimum Sustainable Price Analysis: Q1 2023," National Renewable Energy Laboratory, Golden, CO, USA, Technical Report NREL/TP-7A40-87303, Nov. 2023.

[22] M. Spiller *et al.*, "A Model-Aware Comprehensive Tool for Battery Energy Storage System Sizing," *Energies*, vol. 16, no. 18, Sep. 2023, Art. no. 6546, https://doi.org/10.3390/en16186546.

[23] M. Moncecchi, C. Brivio, S. Mandelli, and M. Merlo, "Battery Energy Storage Systems in Microgrids: Modeling and Design Criteria," *Energies*, vol. 13, no. 8, Apr. 2020, Art. no. 2006, https://doi.org/10.3390/en13082006.

[24] A. A. Heidari, S. Mirjalili, H. Faris, I. Aljarah, M. Mafarja, and H. Chen, "Harris hawks optimization: Algorithm and applications," *Future Generation Computer Systems*, vol. 97, pp. 849–872, Aug. 2019, https://doi.org/10.1016/j.future.2019.02.028.

[25] R. W. Ferrero, S. M. Shahidehpour, and V. C. Ramesh, "Transaction analysis in deregulated power systems using game theory," *IEEE Transactions on Power Systems*, vol. 12, no. 3, pp. 1340–1347, Dec. 1997, https://doi.org/10.1109/59.630479.

[26] D. Cao *et al.*, "Bidding strategy for trading wind energy and purchasing reserve of wind power producer – A DRL based approach," *International Journal of Electrical Power & Energy Systems*, vol. 117, Oct. 2019, Art. no. 105648, https://doi.org/10.1016/j.ijepes.2019.105648.

[27] A. Vitina *et al.*, "IEA Wind Task 26: Wind Technology, Cost, and Performance Trends in Denmark, Germany, Ireland, Norway, the European Union, and the United States: 2007–2012," National Renewable Energy Laboratory, Technical Report NREL/TP-6A20-64332, June 2025.

[28] T. V. Anh, N. T. Linh, and D. N. Sang, "Controlling Output Power to Enhance the Investment Efficiency of Wind Farms by Maximizing the Capacity of Transmission Transformers and Integrating Energy Storage Systems," *Engineering, Technology & Applied Science Research*, vol. 14, no. 4, pp. 15751–15756, Aug. 2024, https://doi.org/10.48084/etasr.7688.